Investigation of Structural, Electronic, and Thermodynamic Properties of The Carvacrol Molecule in Gas Phase and Different Solvents

Fatma Genç [1], Fatema Tayfour [2], Fatma Kandemirli [3]

[1] Department of Pharmaceutical Chemistry, Faculty of Pharmacy, Istanbul Yeni Yuzyil University, Istanbul, Turkey
Email: ftmgenc@yahoo.com

[2] Biomedical Engineering Department, Faculty of Engineering & Architecture, Kastamonu University, Kastamonu, Turkey
Email: fatematayfour0@gmail.com

[3] Biomedical Engineering Department, Faculty of Engineering & Architecture, Kastamonu University, Kastamonu, Turkey
Email: fkandemirli@yahoo.com

Article History

Received: Jul. 17, 2025

Revised: Oct. 04, 2025

Accepted: Jul. 11, 2025

Abstract

The electronic structure and some thermodynamic properties of Carvacrol molecule were investigated in detail with calculations at MP2/6-311G(d,p) level in environments such as gas, n-octanol, acetone, ethanol, acetonitrile, DMF, water. The effects of different environments on electron-filled HOMO, HOMO-1, HOMO-2, HOMO-3, and electron-empty LUMO, LUMO+1, LUMO+2, LUMO+3, which are close to the frontier orbitals, and also on polarizability, hyperpolarizability, and thermodynamic parameters of the molecule were investigated. It was observed that highly polar solvents significantly affected the electron density and stability of Carvacrol molecule. It was found that the electronic structure and optical properties of Carvacrol molecule were affected by the solvent environment. Findings about NLO properties and electronic properties of Carvacrol molecule in different environments provide important information in optoelectronic and pharmaceutical applications.

Keywords- Carvacrol properties, Frontier Orbitals, MP2/6-311G(d,p), Thermodynamic Properties.

I. INTRODUCTION

Carvacrol (2-Methyl-5-(propan-2-yl)phenol), found in the essential oils of thyme and similar plants, is a biologically active phenolic monoterpene. A natural compound, Carvacrol attracts attention due to its antiviral, antibacterial, anti-inflammatory and antioxidant properties. Numerous in vitro and in vivo studies in recent years have shown that this compound is of increasing importance in medical and industrial fields (1), (2). The effects of carvacrol on gastrointestinal microbiota have been examined in in vitro studies, and it has been revealed that it exhibits significant antimicrobial activity against both beneficial and harmful intestinal bacteria. However, due to its pharmacokinetic properties, its therapeutic efficacy in the intestinal environment may be limited. Therefore, the development of controlled release systems plays a critical role in increasing the effectiveness of carvacrol (3).

Carvacrol shows its antibacterial effect by disrupting the bacterial membrane, inhibiting resistance pumps and preventing biofilm formation. In addition, it interrupts bacterial communication by suppressing the Quorum Sensing mechanism these properties, can reduce the dosage requirement by showing synergistic interaction with antibiotics. When formulated with nano and polymer-based carrier systems, its effectiveness in biofilm targeting increases and its potential for clinical applications is strengthened (4). On the other hand, the low water solubility and limited bioavailability of carvacrol limit its therapeutic applications. However, innovative carrier systems such as zein-based nanoparticles stabilized with lecithin, molecular interactions are increased and effective transport to target cells is provided. These nanoparticles show cytotoxic effects on colon cancer cells and promise promise by facilitating intracellular internalization (5).

The antiviral potential of carvacrol was revealed especially by molecular binding analyses performed on the SARS-CoV-2 Omicron variant. These studies show that high-affinity binding of carvacrol with the spike protein and the main protease enzyme can prevent the virus from entering the cell and replication processes. However, advanced in vitro and in vivo studies are needed to confirm these findings (6).
In addition, the strong effect of carvacrol among alpha-glucosidase inhibitors allows it to be recommended as a natural and effective alternative in the treatment of diabetes (7). It has shown protective effects in ethanol-induced gastric ulcer models thanks to its antioxidant and anti-inflammatory properties (8).
The role of carvacrol in cancer treatment is increasingly gaining importance. Carvacrol/chitosan nanoparticles exhibited synergistic anticancer effects with topoisomerase inhibitors in breast and cervical cancer cells, and their combination with doxorubicin increased the treatment efficacy (9). In addition, biomaterials containing carvacrol contribute to the prevention of implant infections and the promotion of wound healing by providing antibacterial properties in 3D printed PLA scaffolds (10). In the treatment of cognitive disorders, the antioxidant and antiapoptotic effects of carvacrol reduce hippocampal neuronal damage and improve learning and memory functions (11).
Finally, computational studies support that the stability of carvacrol-containing essential oils can be increased with B12N12 nanocages against increasing antibiotic resistance, thus increasing their biological activities (12). The solubility and molecular interactions of carvacrol have been studied in detail in various organic solvents. The determination that carvacrol is soluble in ethanol, diethyl ether and alkaline solvents and especially well soluble in acetone, but its solubility in water is quite low, directly affects the applications of carvacrol in the food industry and pharmaceuticals.
(13), (14). Nanoformulations containing carvacrol and thymol have been shown to increase the solubility of carvacrol and enhance its efficacy. Their antibacterial effects have also been investigated. Supporting the potential use of nanoformulations containing carvacrol and thymol in pharmaceutical and food protection (15).
They designed and synthesized a series of carvacrol-based thiosemicarbazide and 1,3,4-thiadiazole-2-amine and conducted extensive molecular docking analysis to show details of interactions between the ligand and the enzyme. They designed and synthesized a series of carvacrol-based thiosemicarbazide and 1,3,4-thiadiazole-2-amine and conducted extensive molecular docking analysis to show details of interactions between the ligand and the enzyme (16).
They synthesized and characterized and done UV–vis spectroscopic analysis a series of novel carvacrol Schiff base complexes with Co (II), Ni (II), Cu (II), and Zn (II) viz. CoB, NiB, CuB, and ZnB and they observed observed for Schiff base is at353.61 nm to a π–π^* transition. And they repoted the valuesare in accordance with the experimental one, i.e., 362 nm (17).
They synthesize new 2,4-substituted halogen derivatives of carvacrol as a starting scaffold for new biologically active compounds and DFT calculations were performed for carvacrol and 2,4-fluoro substituted carvacrol (18).
They studied the antiradical properties of eugenol, safrole, myristicin, carvacrol, cinnamalde-hyde, and isoeugenol found in antioxidant essential oils, and studied molecular descriptors, frontiermolecular orbitals, and molecular electrostatic potential have been studied by using density functional theory (19).
These studies demonstrate that carvacrol is a promising compound in the pharmaceutical, food, and medical fields due to its diverse biological activities and the formulations developed using carrier systems. Nonetheless, additional research is required to evaluate its clinical applicability and ensure safety.
In this study, the electronic and structural properties of the carvacrol molecule were investigated in detail by quantum chemical calculations. The three-dimensional structure of the molecule was modeled with the GaussView program and the geometry optimization was performed using the Gaussian software at the MP2/6-311G(d,p) level. After optimization, the energy levels of HOMO, LUMO and related orbitals and electrostatic potential distributions, dipole moment and various thermodynamic parameters (total energy, enthalpy, free energy, etc.) were calculated. In addition, solvent effects were evaluated comparatively with calculations performed in different solvent environments and theoretical data on the reactivity and stability of the molecule were obtained.

II. MATERIALS AND METHODS

The structure of the carvacrol molecule used in this study was drawn with the help of the GaussView program and transferred to the Gaussian software for optimization. The geometry optimization of the molecule in the gas phase was carried out using the MP2 level and the 6-311G(d,p) basis set. As a result of the quantum chemical calculations made on the structure; parameters such as HOMO, LUMO and related orbital energy levels, electrostatic potential distributions (ESP), dipole moment, total electronic energy, zero-point energy, thermal energy, enthalpy, free energy, Mulliken charge distributions and bond lengths were obtained.
All calculations were carried out using a workstation with high processing capacity. Graphical analyzes were made in line with the obtained data and the solvent effects were evaluated comparatively for various environments (gas, n-octanol, acetone, ethanol, acetonitrile, DMF and water).

III. RESULT AND DISCUSSION

A. Optimization and Electronic Orbital Views (HOMO, LUMO, ESP) of the Carvacrol Molecule in the Gas Phase

The optimized form of the Carvacrol molecule in the gas phase using the 6-311G(d,p) basis set at the MP2 level, and the HOMO, HOMO-1, HOMO-2, HOMO-3, LUMO, LUMO+1, LUMO+2, LUMO+3 and ESP views are given in Figure 1.

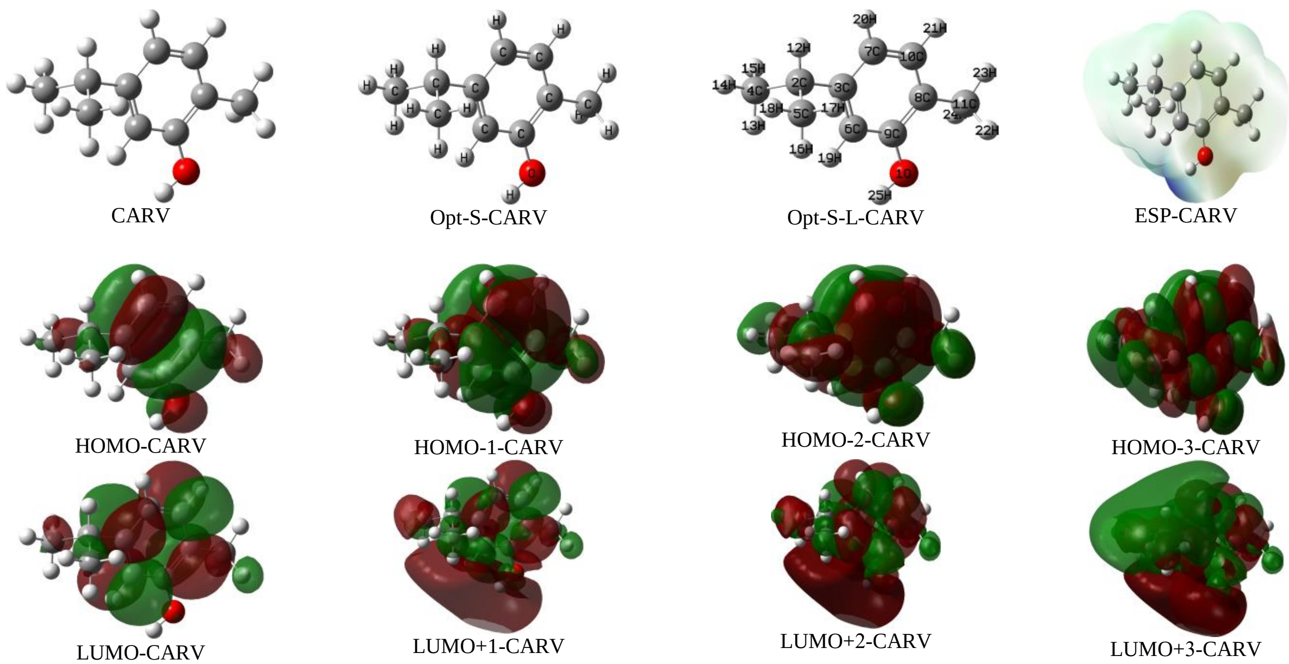

Figure 1. HOMO, HOMO-1, HOMO-2, HOMO-3, LUMO, LUMO+1, LUMO+2, LUMO+3, and ESP of carvacrol molecule

Considering different solvent environments (gas (ε = 0), n-octanol (ε = 9.86), acetone (ε = 20.49), ethanol (ε = 24.85), acetonitrile (ε = 35.69), DMF (ε = 37.22), water (ε = 78.36)), detailed analyses were performed on the frontier orbital structures and electrostatic properties of the carvacrol molecule.

The molecular orbitals of the carvacrol molecule provide comprehensive information on its electronic structure and reactivity. HOMO is completely delocalized on the aromatic π system and shows high electron density in the region close to the phenolic –OH group (19). This indicates that the molecule has a pronounced nucleophilic character and a strong electron donor ability. HOMO-1 is similarly concentrated on the hydroxyl group and aromatic ring, indicating its potential contribution in charge transfer processes. HOMO-2 has an asymmetric localization in the region substituted by the methyl group, which is important in terms of local reactivity in special cases. HOMO-3, on the other hand, is largely delocalized, has a structure with low direct reactivity but contributes to the electronic stability of the molecule.

LUMO, on the other hand, is spatially concentrated in different regions compared to HOMO and represents electron-poor areas far from the –OH group, indicating suitable target areas for electrophilic attack. The empty orbitals at higher energy levels (LUMO+1–LUMO+3) have the potential for excited state polarizations and optical properties, showing increased asymmetry and broadening between aromatic/non-aromatic regions.

In addition to the orbital distributions described above, the color distribution observed along the ESP surface clearly revealed the different electrostatic regions located on the surface of the molecule. Electron-rich (red) areas are localized especially around the hydroxyl oxygen and define this region as the primary nucleophilic center. Electron-poor (blue) areas are particularly evident around hydrogen atoms attached to the methyl and hydroxyl groups; these regions are evaluated as potential electrophilic attack centers. In the aromatic ring, a moderately balanced potential is observed due to delocalized π electrons. The general dipolar orientation of the molecule is from the –OH group to the opposite end, which is suitable for hydrogen bonds, π–π stacking and other weak interactions. These features support the physicochemical character of carvacrol, which can play a decisive role in its interactions with biological systems.

B. Change in Frontier Orbital Atomic Contributions of the Carvacrol Molecule Depending on the Polarity of Solvent Environments

Tables 1 and 2 show the percentages of atoms contributing to the HOMO and LUMO orbitals in the gas phase of the Carvacrol molecule. These data reveal which atoms play a more active role in the highest occupied and lowest occupied molecular orbitals of the molecule and provide information about the localization of molecular reactivity. Only contributions above 2% were taken into account in the analyses, thus atoms with significant effects on the orbital structure were highlighted.

TABLE I. CONTRIBUTIONS OF ATOMIC ORBITALS OF THE CARVACROL MOLECULE TO HOMO HOMO-1 HOMO-2 HOMO-3

HOMO							
Atoms	***Gas***	***n-octanol***	***Acetone***	***Ethanol***	***Acetonitrile***	***DMF***	***Water***
O1	6.78	6.88	6.9	6.9	6.9	6.9	6.91
C3	16.51	16.16	16.12	16.12	16.11	16.11	16.1
C7	25.58	25.95	25.98	25.98	25.99	25.99	26
C8	24.01	24	24	24.01	24	24	24
C9	18.96	18.87	18.86	18.85	18.86	18.86	18.85
HOMO-1							
O1	2.21	2.26	2.27	2.27	2.27	2.27	2.28
C3	9.04	9.54	9.59	9.59	9.61	9.61	9.63
C6	36.31	36.32	36.32	36.32	36.31	36.31	36.31
C7	6.2	5.81	5.77	5.77	5.76	5.76	5.75
C8	8.83	8.78	8.77	8.77	8.77	8.77	8.77
C9	4.89	5.04	5.06	5.06	5.06	5.06	5.07
C10	28.69	28.31	28.26	28.25	28.25	28.24	28.23
HOMO-2							
O1	9.2	8.46	8.36	8.34	8.31	8.31	8.28
C2	7.78	9.68	9.94	9.98	10.05	10.06	10.14
C3	8.87	7.3	7.1	7.07	7.01	7.01	6.95
C4	6.73	8.32	8.54	8.57	8.63	8.64	8.7
C5	6.73	8.32	8.54	8.58	8.64	8.64	8.71
C6	9.11	7.72	7.54	7.52	7.47	7.47	7.41
C7	15.03	13.67	13.48	13.45	13.39	13.39	13.33
C8	9.2	8.46	8.36	8.34	8.31	8.31	8.28
C9	7.78	9.68	9.94	9.98	10.05	10.06	10.14
C10	8.87	7.3	7.1	7.07	7.01	7.01	6.95
C11	6.73	8.32	8.54	8.57	8.63	8.64	8.7
H15	6.73	8.32	8.54	8.58	8.64	8.64	8.71
H17	9.11	7.72	7.54	7.52	7.47	7.47	7.41
HOMO-3							
C2	17.08	17.95	18.05	18.07	18.1	18.1	18.14
C3	13.93	13.29	13.2	13.2	13.15	13.14	13.11
C4	8.69	9.76	9.88	9.9	9.94	9.94	9.98
C5	8.69	9.75	9.88	9.89	9.93	9.94	9.98
C6	4.03	3.74	3.71	3.71	3.7	3.69	3.68
C7	8.33	7.99	7.94	7.94	7.92	7.92	7.91
C8	4.09	3.48	3.41	3.4	3.38	3.38	3.36
C9	17.08	17.95	18.05	18.07	18.1	18.1	18.14
C10	13.93	13.29	13.2	13.2	13.15	13.14	13.11
C11	8.69	9.76	9.88	9.9	9.94	9.94	9.98
H14	8.69	9.75	9.88	9.89	9.93	9.94	9.98
H18	4.03	3.74	3.71	3.71	3.7	3.69	3.68
H19	8.33	7.99	7.94	7.94	7.92	7.92	7.91
H21	4.09	3.48	3.41	3.4	3.38	3.38	3.36

TABLE II. CONTRIBUTIONS OF ATOMIC ORBITALS OF THE CARVACROL MOLECULE TO LUMO, LUMO+1, LUMO+2, AND LUMO+3

LUMO								
Atoms		***Gas***	***n-octanol***	***Acetone***	***Ethanol***	***Acetonitrile***	***DMF***	***Water***
C2		2.58	2.42	2.4	2.4	2.39	2.39	2.39
C3		17.07	16.77	16.75	16.75	16.74	16.74	16.74
C6		23.87	24.08	24.11	24.11	24.11	24.11	24.12
C8		17.75	17.71	17.71	17.71	17.71	17.71	17.72
C9		2.79	2.7	2.69	2.69	2.68	2.68	2.68
C10		28.87	29.35	29.4	29.41	29.41	29.42	29.43
LUMO+3								
H12		25.56	17.85	16.56	16.35	16	15.96	15.57
H14		18.03	10.73	9.98	9.87	9.68	9.66	9.45
H15		9.27	6.38	6.05	6.01	5.92	5.91	5.82
H17		9.27	6.39	6.05	6.01	5.92	5.91	5.82
H18		18.03	10.73	9.98	9.87	9.68	9.66	9.45
H19		-	3.73	3.63	3.59	3.53	3.53	3.44
H20		15.86	10.08	9.08	8.92	8.65	8.62	8.32
H22		-	8.96	10.74	11.05	11.57	11.62	12.22
H23		-	3.84	5	5.21	5.56	5.59	6.01
H24			8.95	10.74	11.05	11.57	11.62	12.22
H25		24.93	39.46	39.42	39.33	39.21	39.19	38.97
LUMO+1								
Atoms	***Gas***	***Atoms***	***n-oktanol***	***Asetone***	***Ethanol***	***Acetonitrile***	***DMF***	***Water***
H13	8.11	**O_1**	2.05	2.06	2.06	2.06	2.06	2.06
H14	3.69	**C_3**	15.47	15.52	15.52	15.53	15.53	15.54
H15	2.81	**C_6**	3.24	3.24	3.24	3.24	3.24	3.24
H16	8.11	**C_7**	27.79	27.79	27.79	27.79	27.79	27.79
H17	2.81	**C_8**	8.51	8.52	8.52	8.53	8.53	8.53
H18	3.69	**C_9**	28.62	28.65	28.66	28.66	28.66	28.67
H19	40.75	**C_{10}**	5.16	5.14	5.14	5.14	5.13	5.13
H20	3.68		-	-	-	-	-	-
H21	47.98		-	-	-	-	-	-
LUMO+2								
O1	2.02	**H_{12}**	8.09	8.89	9.01	9.22	9.24	9.46
C3	14.88	**H_{13}**	9.34	9.16	9.12	9.07	9.07	9
C6	3.28	**H_{14}**	9.66	10.24	10.32	10.46	10.48	10.63
C7	27.81	**H_{15}**	7.59	8.19	8.29	8.45	8.46	8.64
C8	8.3	**H_{16}**	9.34	9.16	9.12	9.07	9.07	9
C9	28.4	**H_{17}**	7.59	8.19	8.29	8.45	8.46	8.64
C10	5.41	**H_{18}**	9.66	10.24	10.32	10.46	10.48	10.63
	-	**H_{19}**	28.98	27.25	26.96	26.52	26.48	25.97
	-	**H_{20}**	9.93	10.74	10.87	11.08	11.1	11.33
	-	**H_{21}**	2.44	2.76	2.82	2.9	2.91	3.01
	-	**H_{22}**	2.39	2.49	2.52	2.54	2.55	2.58
	-	**H_{23}**	2.39	2.49	2.52	2.54	2.55	2.58
	-	**H_{24}**	24.3	22.15	21.84	21.29	21.24	20.65

As seen in Table 1, carbon atoms such as C7, C8 and C6 provide significant contributions in the HOMO, HOMO-1, HOMO-2 and HOMO-3 orbitals. While C7 and C8 atoms provide high and relatively stable contributions, it is seen that C6 atom plays a dominant role in the HOMO-1 level, regardless of the solvent. The contribution distribution becomes more complex in the HOMO-2 and HOMO-3 levels, and while the contribution of the O1 atom decreases in highly polar solvents, an increase in the contributions of certain carbon atoms is observed. These findings clearly reveal the effects of the solvent environment on the electronic structure and orbital stability of the molecule.

Table 2 shows the atomic contributions of LUMO, LUMO+1, LUMO+2 and LUMO+3. It was determined that especially C6 and C10 atoms play important roles as electron acceptors at these levels and that solvent polarity partially increases these contributions. In addition, significant contributions from hydrogen atoms to the LUMO+ orbitals are found, indicating that the antibonding character of these orbitals is susceptible to change due to solvent effects. In particular, a general decrease in the contributions from hydrogen atoms at the LUMO+3 level is observed as the solvent polarity increases, suggesting that the orbitals at these higher energy levels are less stable in polar solvents.

TABLE III. HOMO, LUMO ENERGY AND ENERGY GAP VALUE

	E_{HOMO}	E_{LUMO}	ΔE
Gas	-8.191	3.647	11.837
n-octanol	-8.334	3.523	11.857
Acetone	-8.354	3.505	11.859
Ethanol	-8.357	3.502	11.859
Acetonitrile	-8.363	3.498	11.860
DMF	-8.363	3.497	11.860
Water	-8.369	3.492	11.861

When we go from gas phase to solvent phase for gas, n-octanol, acetone, ethanol, acetonitrile, DMF and water E_{HOMO} increases as negative value 1.717%, 1.954%, 1.989%, 2.056 %,2.062%, 2.135% supports solvent dielectric constant increases, the E_{HOMO} becomes more negative (20, 21). When we go from gas phase to solvent phase for gas, n-octanol, acetone, ethanol, acetonitrile, DMF and water E_{LUMO} decrease.

C. Investigation of Nonlinear Optical (NLO) Parameters of the Carvacrol Molecule in Different Solvent Environments

Figure 2 shows the comparison of polarizability%, anisotropic polarizability and hyperpolarizability values of carvacrol molecule in different solvents (gas, n-octanol, acetone, ethanol, acetonitrile, DMF, water).

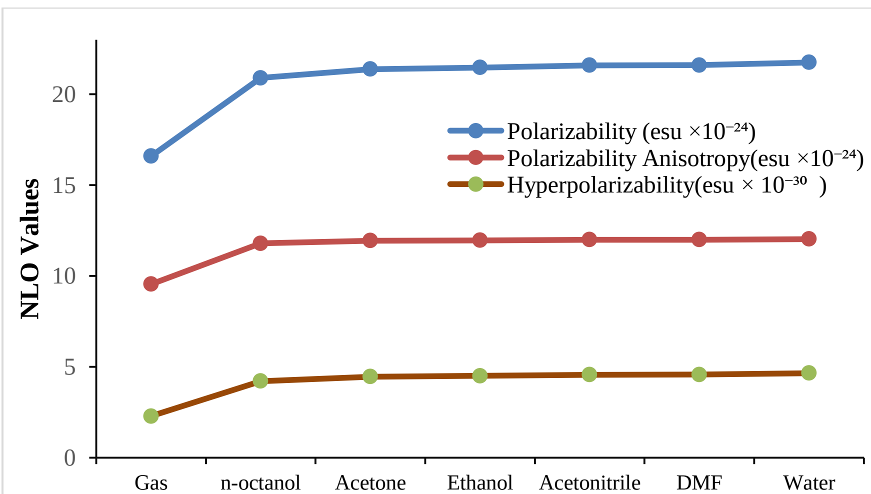

Figure 2. NLO values of the Carvacrol molecule

A significant increase is observed in all nonlinear optical (NLO) parameters with the increase in the dielectric constant of the solvent medium (especially from n-octanol to water). The highest values were obtained in the high polarity water medium. This shows that the carvacrol molecule exhibits stronger dipole interactions in highly polar solvents and its suitability for optoelectronic applications increases.

It has the lowest polarizability, hyperpolarization, and anisotropy because there is no external stabilization of charge distribution. Although n-octanol is less polar, there is a significant increase (26.77% higher) in the nonpolar solvent n-octanol compared to the gas phase, as it provides some dielectric stabilization of electron density and increases electron cloud delocalization due to solvent-solute dispersion and hydrogen bonding with the hydroxyl group. The polarizability, anisotropic polarizability and hyperpolarizability values of carvacrol increase consistently with the increase in solvent polarity, and this increase reveals that the electron cloud of the molecule is more deformed by the solvent effect. While the values in the gas phase (e.g. polarizability: 16.592×10^{-24} esu) remain low compared to other solvents, the polarizability reaches the maximum value (21.756×10^{-24} esu) in highly polar solvents such as water. Anisotropic polarizability and hyperpolarizability values are also at the highest level with 12.037 and 4.656, respectively.

Both the average polarizability and the first hyperpolarizability (β) of a molecule generally increase as the solvent dielectric constant increases, because a high dielectric medium more effectively stabilizes charge-separated resonance forms, leading to stronger intramolecular charge transfer between electron-donating and electron-accepting regions. In polar solvents, stabilization of dipolar or charge-transfer states allows the molecule's electronic cloud to be more easily disrupted by an external electric field, increasing polarizability and, therefore, hyperpolarizability (22, 23).

D. Investigation of the Dipole Moment Behavior of the Carvacrol Molecule in Different Solvents

Figure 3 displays the variations in the dipole moment of the carvacrol molecule across different solvents.

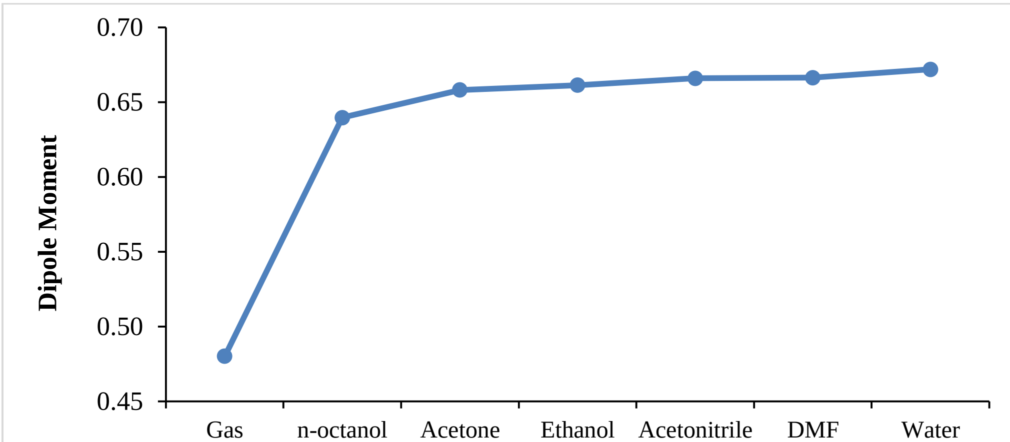

Figure 3. Dipole Moment of the Carvacrol Molecule

Figure 3 shows the dipole moment changes of carvacrol molecule in different solvents. The dipole moment was measured at the lowest level (0.48 Debye) in the gas phase, and a regular and gradual increase in dipole moment values was observed as the solvent polarity increased. There is a significant increase especially after n-octanol and the maximum value of 0.672 Debye is reached in the water environment. The dipole moment of carvacrol molecule in gas, gas, n-octanol, acetone, ethanol, acetonitrile, DMF, water are 0.4802, 0.6397, 0.6581, 0.6613, 0.6659, 0.6664, 0.6719, so dipole moment increases. According to the basic electrostatic mechanism, electron density redistributes, so the molecular dipole generally increases in more polar solvents (22).

The environmental electric field created by the solvent molecules has an increasing effect on the electron distribution of carvacrol. This increase, observed in solvents with high polarity, especially those that can form hydrogen bonds, is related to the structural flexibility of the molecule and its electronic response to the external environment. The increasing dipole moment reveals that the charge distribution and dipole character of carvacrol are significantly affected by the solvent polarity, thus making the molecule more sensitive to external electric fields and other dipoles.

E. Changes in Electronic and Thermodynamic Energy Values of Carvacrol Molecule in Different Solvent Environments with Solvent Polarity

It is revealed that the values of the sum of electronic and zero-point energies (E_{EZPE}), sum of electronic and thermal energies (E_{ETP}), sum of electronic and thermal enthalpies (En_{ETP}) and sum of electronic free energies (GET) of the carvacrol molecule show a low but continuous decrease as the solvent polarity increases (Figure 4).

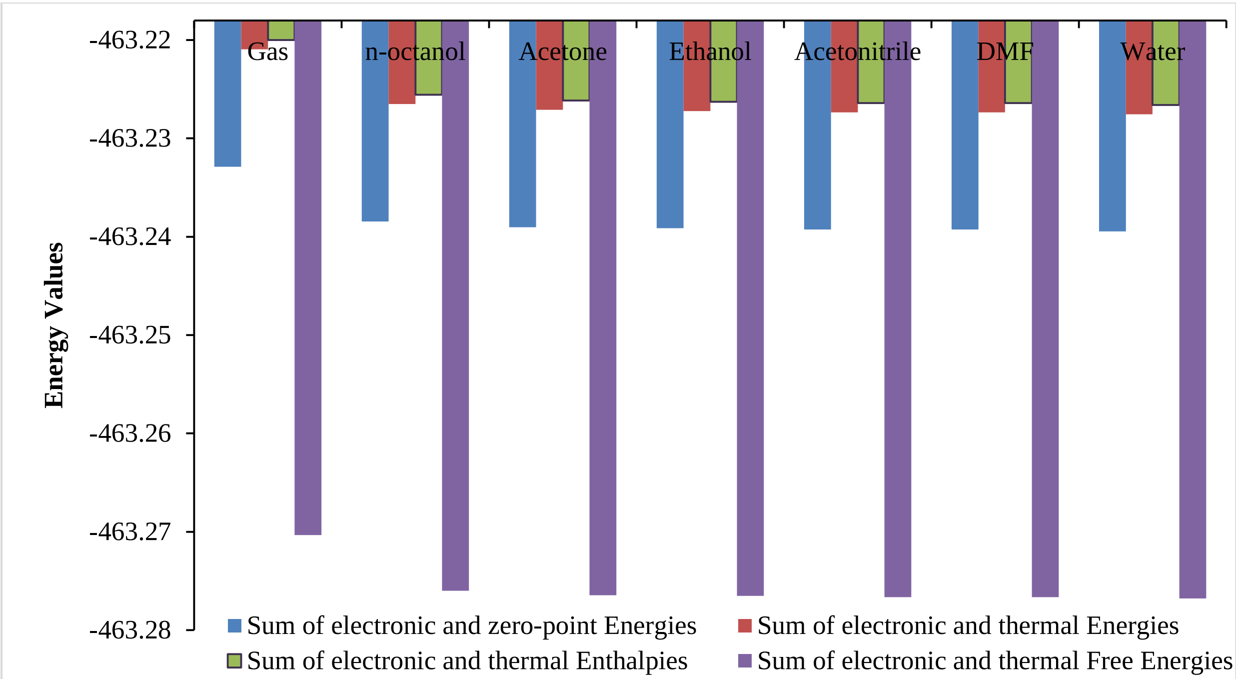

Figure 4. Electronic total energy, zero-point energy, thermal energy, thermal enthalpy and thermal free energy values of the carvacrol molecule (in au units)

While these energy values are at the highest level (less stable) in the gas phase, they reach the lowest levels (more stable) in solvents with high polarity — especially in water and DMF environments.

This situation shows that the carvacrol molecule gains a more stable structure in the solvent environment and that interactions with solvent molecules stabilize the total energy profile of the molecule. In particular, the decrease in thermal free energy indicates that the molecule is thermodynamically more favorable and more resistant to reactions in the solvent.

F. Stability and Changes in Bond Lengths of Carvacrol Molecule in Solvent Environments

When Figure 5 is examined, it is seen that the bond lengths of the carvacrol molecule optimized in different solvent environments remain largely constant and exhibit only very small changes. In particular, minimal elongations of ±0.001–0.002 Å were observed on average in the C–C bonds within the aromatic ring due to the effect of solvent, which revealed that the ring structure has high structural stability against solvent effects. Similar limited changes were reported in non-ring bonds such as C8–C11, C3–C2. The C9–O1 bond showed a slight shortening tendency against solvent polarity, suggesting that the hydroxyl group is more sensitive to interactions.

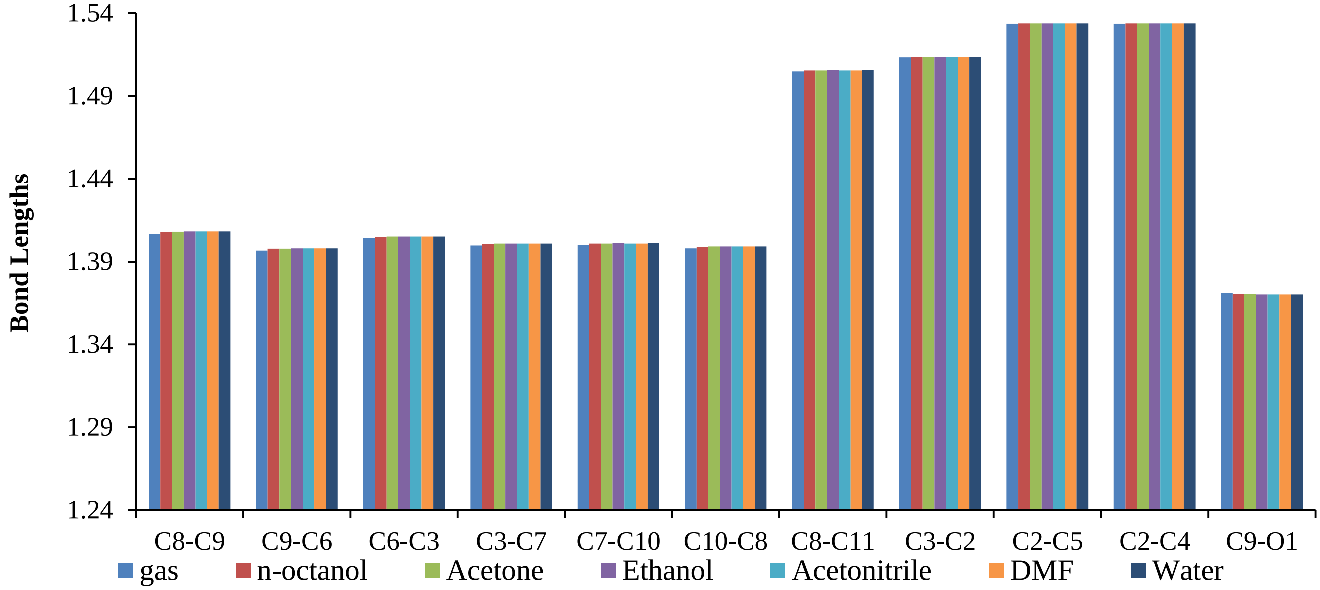

Figure 5. Bond length of the Carvacrol molecule in different solvents

G. Effect of Solvent Polarity on Mulliken Charge Distribution in the Carvacrol Molecule

Figure 6, created according to the results of Mulliken charge analysis performed at the MP2/6-311G(d,p) level, clearly reflects the changes in the atomic charge distribution of the carvacrol molecule in different solvent environments.

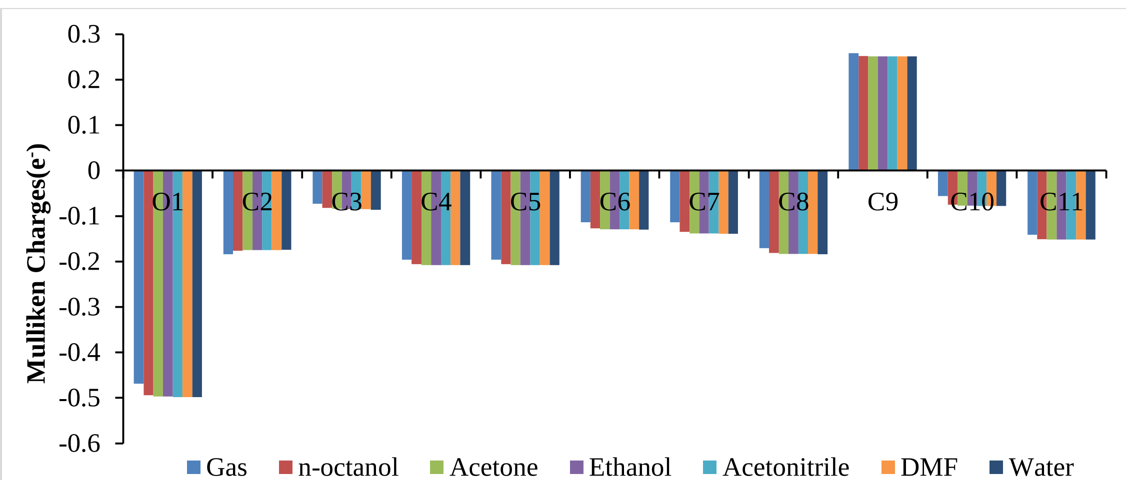

Figure 6. Mulliken charge distribution changes of the Carvacrol molecule in the gas phase and in n-octanol, acetone, ethanol, acetonitrile, DMF and water solvents.

Figure 6 shows that significant electronic density changes occur in some atoms, especially with the increase in solvent polarity. The charge of the O1 oxygen atom tends to shift to more negative values in all solvents, starting from the gas phase. This suggests that polar solvents increase the electron density around the O1 atom through hydrogen bonds and dipole-dipole interactions, further stabilizing the negative charge in this region. It is observed that this effect is more pronounced, especially in highly polar solvents such as water, DMF and acetonitrile.

Although the Mulliken charge changes observed in carbon atoms are relatively limited, it is understood that negativity increases or positivity decreases in some atoms due to the solvent effect. The fact that the charges in the C3, C4, C5, C6, C7, C8, C10 and C11 atoms tend towards more negative values suggests that the solvents increase the electron density in these regions and make the atoms more electronegative. The changes recorded in the C7, C8 and C10 atoms are particularly striking; the fact that these atoms are located close to the functional groups causes them to be more open to the solvent effect.

However, a slight increase in positive charge was determined in the C2 atom; this indicates that the electron density around this center has decreased. The C9 atom is the only center carrying a positive charge and showed a slight decrease in the charge value due to the solvent effect. This shows that the atom maintains its positivity but has decreased to a relatively lower level.

H. Comparison of Total and Vibrational Thermal Energy Values of Carvacrol Molecule in Different Solvent Environments

The relationship between total thermal energy (Total E) and vibrational thermal energy (Vibrational E) of Carvacrol molecule in different solvent environments is shown comparatively. (Figure 7).

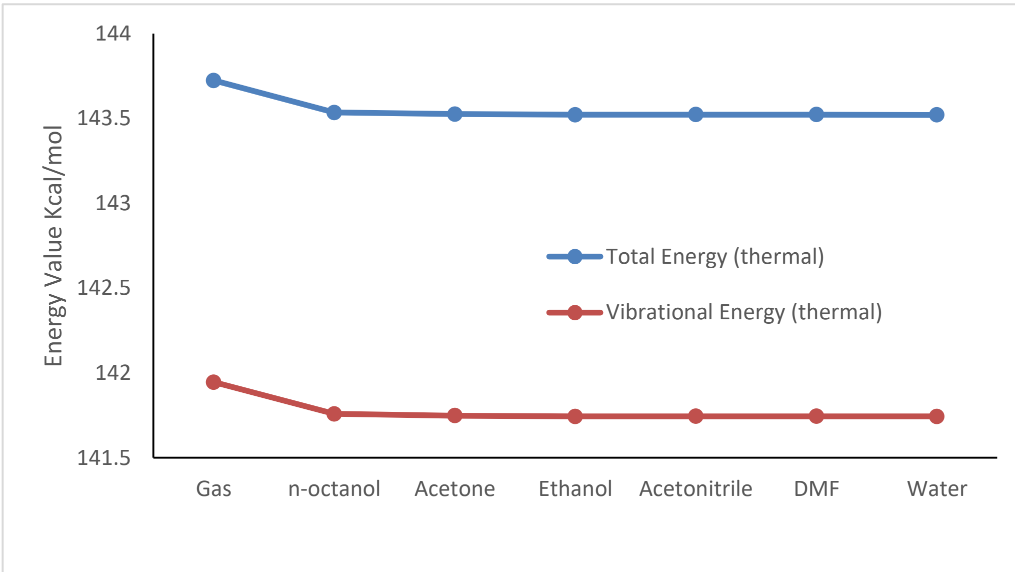

Figure 7. Relationship between total thermal energy (Total E) and vibrational thermal energy (Vibrational E)

The most striking feature in the figure is that both types of energy are very close to each other and the lines run parallel to each other. This suggests that the molecular structure of carvacrol changes only to a limited extent in the distribution of thermal energy in different solvent environments.

The highest total thermal energy (143.723 kcal/mol) and vibrational thermal energy (141.945 kcal/mol) values observed in the gas phase indicate that the carvacrol molecule has higher energy in the environment where it is in the free state. These high energy levels indicate that the free vibrations and movements of the molecule occur at a maximum independent of the solvent effect.
Total thermal energy (Total E) is the sum of vibrational, translational, and rotational contributions. As seen in Figure 7, because carvacrol is a large molecule with many vibrational modes, vibrational energy dominates (more than 98.76%). The constant difference between Total E and Vibrational E (~1.78 kcal/mol) supports the notion that it corresponds to constant translational and rotational contributions that are solvent-independent. Solvents cause only very small shifts in vibrational thermal energy, slightly reducing both values (24).

I. Entropy and Vibrational and Total Heat Capacity Values of the Carvacrol Molecule in gas and Different Environment

Figure 8 compares the thermodynamic parameters-specific heat capacity and entropy-of the carvacrol molecule in various solvents.

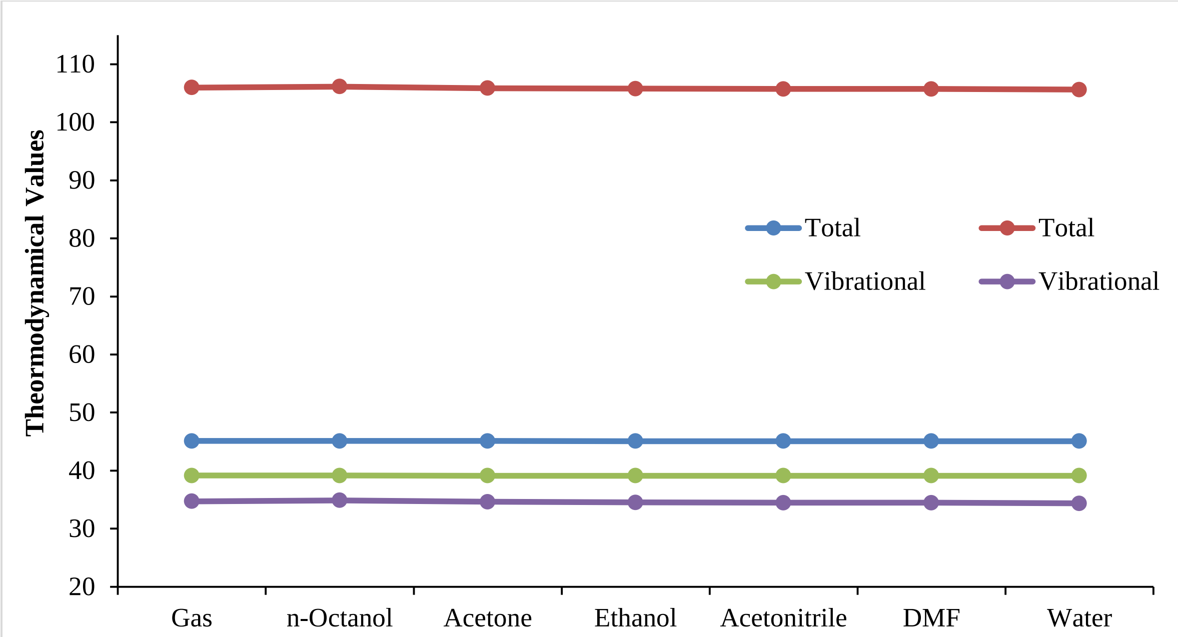

Figure 8, Entropy and vibrational and total heat capacity values of the carvacrol molecule in different solvents

In Figure 8, the vibrational and total heat capacity and entropies of the carvacrol molecule in environments such as gas, n-octanol, acetone, ethanol, acetonitrile, DMF, and water are given. The vibration component is calculated from the vibration frequencies (harmonic oscillator expressions). Resolver models (PCM, SMD, etc.) cause the frequencies to change, especially in H-coupled or low-frequency torsional modes (25).
Vibrational entropy is used to explain solvent-dependent flexibility, to understand stabilization from hydrogen bonding and π–π , and to compare conformers or docking geometries (26).

The total entropy values of carvacrol molecule are 105.974, 106.149, 105.887, 105.792, 105.738, 105.729, 105.615 cal/mol.K in gas, n-octanol, acetone, ethanol, acetonitrile, DMF, and water phases, respectively. It is maximum in n-octanol solvent. The slight decrease in entropy values as the solvent polarity increases can be explained by the decrease in conformational diversity of the molecule and the restriction of its degrees of freedom.

IV. CONCLUSION

In this study, the structural, electronic and thermodynamic changes of the carvacrol molecule in gas, n-octanol, acetone, ethanol, acetonitrile, DıMF and water were examined in detail by quantum chemistry methods and the results obtained explain that the solvent polarity has decisive effects on the HOMO and LUMO energy levels, energy gap (ΔE), dipole moment, polarizability parameters, electrostatic potential distribution and thermodynamic stability of the molecule. Increasing solvent polarity produces a larger induced dipole moment. The reason why n-octanol has the highest entropy and heat capacity among solvents is that, while n-octanol is less polar, its long alkyl chain provides a hydrophobic and less structured environment. The solvent does not strongly "lock" the solute in place, allowing the solute molecule to assume different conformations.
When the distribution of HOMO and LUMO orbitals was examined, high electron density was detected especially in the region where the –OH group was located, and this was an important indicator in determining the reactivity centers of the molecule. For example, C6 atom provide significant contributions in the HOMO-1 with 36.31, 36.32, 36.32, 36.32, 36.31, 36.31, 36.31 and for LUMO-1 28.87, 29.35, 29.4, 29.41, 29.41, 29.42, 29.43 values in Gas, n-octanol, Acetone, Ethanol, Acetonitrile, DMF, Water, respectively. As the solvent environment changes, shifts in the frontier orbital energy levels indicate that the chemical behavior of carvacrol may also change in different environmental conditions. This situation emphasizes the importance of considering environmental factors, especially in applications such as drug delivery systems or biosensor designs. The HOMO-LUMO gap increased by 0.163%, 0.185%, 0.179%, 0.193%, 0.194%, and 0.199% from the gas phase to the solvent phase in polar solvents.
Electrostatic potential maps revealed that the electrophilic and nucleophilic regions of the molecule were reshaped depending on the solvent and it was observed that these regions became more pronounced and the molecule gained a more polar character, especially in polar solvents such as water, DMF. In addition, the increases observed for example value of 0.672 Debye in the water in the dipole

moment and nonlinear optical parameters indicate that carvacrol became more sensitive to external electric fields and could be evaluated for potential optoelectronic applications.

When evaluated from a thermodynamic perspective, it was concluded that carvacrol reached lower free energy values, especially in polar solvents, and this situation provided the molecule with a more stable structure in the solvent environment. This provides important clues about the stability of carvacrol in biological environments (water-based systems) and structural analyses revealed that the basic skeleton of the molecule is resistant to solvent effects and maintains a stable geometry.

In conclusion, this study shows that the chemical and physical properties of the carvacrol molecule are directly related to the solvent environment. Moreover, provides a theoretical basis for future experimental designs, drug delivery systems, biosensors and nanomaterial applications. This study confirmed once again that the choice of solvent can directly affect the interactions at the molecular level and the success in applications.

References

[1] T. Hasanvand, M. Mohammadi, F. Abdollahpour, B. Kamarehie, A. Jafari, A. Ghaderpoori, M. A. Karami, "A comparative study on antibacterial activity of carvacrol and glutaraldehyde on Pseudomonas aeruginosa and Staphylococcus aureus isolates: an in vitro study," J Environ Health Sci Eng, vol. 19, no. 1, pp. 475-482, 2021, doi: 10.1007/s40201-021-00620-1.

[2] M. V. Garg, and B. D. Sahu, "Carvacrol and its effect on cardiovascular diseases: From molecular mechanism to pharmacological modulation," Food Biosci, vol. 57, p. 103444, 2024, doi: 10.1016/J.FBIO.2023.103444.

[3] J. Michiels, J. Missotten, D. Fremaut, S. De Smet, and N. Dierick, "In vitro dose–response of carvacrol, thymol, eugenol and trans-cinnamaldehyde and interaction of combinations for the antimicrobial activity against the pig gut flora," Livest Sci, vol. 109, no. 1-3, pp. 157-160, 2007, doi: 10.1016/J.LIVSCI.2007.01.132.

[4] K. Kachur and Z. Suntres, "The antibacterial properties of phenolic isomers, carvacrol and thymol," Crit Rev Food Sci Nutr, vol. 60, no. 18, pp. 3042–3053, 2020, doi: 10.1080/10408398.2019.1675585.

[5] P. Shinde, H. Agraval, A. K. Srivastav, U. C. S. Yadav, and U. Kumar, "Physico-chemical characterization of carvacrol loaded zein nanoparticles for enhanced anticancer activity and investigation of molecular interactions between them by molecular docking," Int J Pharm, vol. 588, p. 119795, 2020, doi: 10.1016/j.ijpharm.2020.119795.

[6] F. E. Öztürkkan, G. B. Akbaba, and P. Aksu Kılıçle, "In silico Investigation of the Interactions of Thymol and Carvacrol on the Spike Protein of Omicron Variant and MPro Enzyme of Coronavirus," Karadeniz Fen Bilimleri Dergisi, vol. 14, no. 3, pp. 997–1005, 2024, doi: 10.31466/kfbd.1338012.

[7] A. Singh, K. Singh, K. Kaur, A. Sharma, P. Mohana, J. Prajapati, U. Kaur, D. Goswami, S. Arora, R. Chadha, P. M. S. Bedi, "Discovery of triazole tethered thymol/carvacrol-coumarin hybrids as new class of α-glucosidase inhibitors with potent in vivo antihyperglycemic activities," Eur J Med Chem, vol. 263, p. 115948, 2024, doi: 10.1016/J.EJMECH.2023.115948.

[8] M. Badr Amira, Naglaa F. El-Orabi, Yasmen F. Mahran, Amul M. Badr, Nervana Mustafa Bayoumy, Hanan Hagar, Elshaymaa I. Elmongy, Reem T. Atawia "In vivo and In silico evidence of the protective properties of carvacrol against experimentally-induced gastric ulcer: Implication of antioxidant, anti-inflammatory, and antiapoptotic mechanisms," Chem Biol Interact, vol. 382, p. 110649, 2023, doi: 10.1016/J.CBI.2023.110649.

[9] A. Akhlaq, M. Ashraf, M. O. Omer, and I. Altaf, "Carvacrol-Fabricated Chitosan Nanoparticle Synergistic Potential with Topoisomerase Inhibitors on Breast and Cervical Cancer Cells," ACS Omega, vol. 8, no. 35, pp. 31826–31838, 2023, doi: 10.1021/acsomega.3c03337.

[10] X. Farto-Vaamonde, L. Diaz-Gomez, A. Parga, A. Otero, A. Concheiro, and C. Alvarez-Lorenzo, "Perimeter and carvacrol-loading regulate angiogenesis and biofilm growth in 3D printed PLA scaffolds," Journal of Controlled Release, vol. 352, pp. 776–792, 2022, doi: 10.1016/J.JCONREL.2022.10.060.

[11] P. Wang, Q. Luo, H. Qiao, H. Ding, Y. Cao, J. Yu, R. Liu, Q. Zhang, H. Zhu, L. Qu, "The Neuroprotective Effects of Carvacrol on Ethanol-Induced Hippocampal Neurons Impairment via the Antioxidative and Antiapoptotic Pathways," Oxid Med Cell Longev, vol. 2017, no. 1, 2017, doi: 10.1155/2017/4079425.

[12] A. Mahal, A. M. Almaamuri, S. S. Noori, S. Chandra, A. Elawady, A. J. Obaidullah, M. H. Shuhata Alubiady, S. H. Zain Al-Abdeen, R. Zainul "Effectiveness of B12N12 Nanocage as a Stabilizer and Delivery Carrier for Thymol and Carvacrol Essential Oils and their Influence on Escherichia coli and Staphylococcus aureus Bacteria: A Comprehensive Analysis using DFT, QTAIM, Multiwfn, and Molecular Docking," Russian Journal of Inorganic Chemistry, vol. 69, no. 9, pp. 1407–1422, 2024, doi: 10.1134/S0036023624601235.

[13] Z. Mohammedi, "Carvacrol: An Update of Biological Activities and Mechanism of Action", Open Access Journal of Chemistry, vol. 1, no. 1, pp. 53-62, 2017, doi: 10.22259/2637-5834.0101008.

[14] H. Chen, P. Michael Davidson, and Q. Zhong, "Impacts of sample preparation methods on solubility and antilisterial characteristics of essential oil components in milk," Appl Environ Microbiol, vol. 80, no. 3, pp. 907–916, 2014, doi: 10.1128/AEM.03010-13.

[15] A. Hajibonabi, M. Yekani, S. Sharifi, J. S. Nahad, S. M. Dizaj, and M. Y. Memar, "Antimicrobial activity of nanoformulations of carvacrol and thymol: New trend and applications," 13, 2023, Elsevier Inc. doi: 10.1016/j.onano.2023.100170.

[16] T. Alagöz, F. G. Çalişkan, H. G. Bilgiçli, M. Zengin, M. Sadeghi, P. Taslimi, İ. Gulçin, "Synthesis, characterization, biochemical, and molecular modeling studies of carvacrol‐based new thiosemicarbazide and 1, 3, 4‐thiadiazole derivatives", Archiv der Pharmazie, vol. 356 no. 12, pp. 2300370, 2023, doi:10.1002/ardp.202300370.

[17] B. R. Salunkhe, E. Soorya, S. S. Pingale, R. Bendre,S. Waghmode, S. Gad, ., "Computational and Experimental Studies on Carvacrol‐Derived Transition Metal Complexes: Structure, Stability, and Biological Activity", ChemistrySelect, vol. 10, no. 28, e00759. 2025, doi:10.1002/slct.202500759.

[18] M. R.Đorđević Zlatković, N. S. Radulović, M. Dangalov & N. G. Vassilev, "Conformation Analysis and Stereodynamics of Symmetrically ortho-Disubstituted Carvacrol Derivatives", Molecules, vol. 29, no. 9, pp. 1962, 2024), doi:10.3390/molecules29091962.

[19] H. Boulebd, "DFT study of the antiradical properties of some aromatic compounds derived from antioxidant essential oils: C–H bond vs. O–H bond", Free Radical Research, vol. 53, no. 11-12, pp. 1125-1134, 2019, doi:10.1080/10715762.2019.1690652.

[20] F. Genç, S. G. Kandemirli, & F. Kandemirli, "Theoretical B3LYP study on electronic structure of contrast agent Iopamidol", Acta Chimica Slovenica, vol. 68, no. 2, pp. 320–331, 2021, doi: 10.17344/acsi.2020.6233.

[21] F. Genç & F. Kandemirli, "Quantum Chemical Calculations of Some Benzene Derivatives", Journal of Amasya University Institute of Sciences and Technology, vol. 1, no. 2, pp. 127–141, 2020,

[22] J. Tomasi, B. Mennucci, & R. Cammi, "Quantum mechanical continuum solvation models", Chemical reviews, vol. 105, no. 8, pp. 2999-3094, 2005, doi: 10.1021/cr9904009

[23] S. G. Kandemirli, F. Genç, F. Kandemirli, & M. Evecen, "Solvent effects on the contrast agent iomeprol with density functional theory", Avrupa Bilim ve Teknoloji Dergisi, vol. 20, pp. 351-359, 2020, doi:10.31590/ejosat.732239.

[24] P. W. Atkins, J. De Paula, & J. Keeler, "Atkins' physical chemistry", Oxford university press. 2023.

[25] Y. Chen, H. Zhang, & Q. Liu, "FT-IR spectroscopy combined with DFT calculation to explore solvent effects of vinyl acetate", Spectrochimica Acta Part A: Molecular and Biomolecular Spectroscopy, vol. 126, pp. 122-128, 2014, doi:10.1016/j.saa.2014.01.105.

[26] L. Chan, G. M. Morris, & G. R. Hutchison, "Understanding conformational entropy in small molecules" Journal of Chemical Theory and Computation, vol. 17, no. 4, pp. 2099-2106, 2021, doi:10.1021/acs.jctc.0c01213.